CHAPTER 16

GROWING THE ANCIENT MAYA SOCIAL-ECOLOGICAL SYSTEM FROM THE BOTTOM UP

SCOTT HECKBERT, CHRISTIAN ISENDAHL, JOEL D. GUNN, SIMON BREWER, VERNON L. SCARBOROUGH, ARLEN F. CHASE, DIANE Z. CHASE, ROBERT COSTANZA, NICHOLAS P. DUNNING, TIMOTHY BEACH, SHERYL LUZZADDER-BEACH, DAVID L. LENTZ, AND PAUL SINCLAIR

Introduction

The rise and fall of civilizations attracts many narratives on the root causes of societal success or failure. Current methods in computational modelling allow us to use archaeological data to build simulation models which test, refute, and help to refine hypotheses on how social-ecological systems function. Archaeological data present numerous examples of how past societies have interacted with the environment and the long- and short-term outcomes of these interactions. Among the most well-studied cases is the ancient Lowland Maya of southern Mesoamerica. The Maya lowlands form a heterogeneous environment in terms of topography, hydrology, soils, vegetation, and climate (Dunning and Beach, 2010). The prehistory of the ancient Maya unfolded over several millennia, developing state polities, urban centres, long-distance exchange networks, advanced technologies, landesque capital, and complex resource management systems by the first millennium BC. The long-term political and economic history of the lowlands suggests a cyclic pattern of regional and subregional growth, decline, and reorganization during the Middle to Late Preclassic (1000 BC-AD 250), Classic (AD 250–900), and Postclassic periods (AD 900–1500). Classic Maya culture reached its height around AD 700 before a rapid and fundamental transformation altered its political, social, economic, and demographic organization. Identifying the causes of this particular reorganization, commonly referred to as the 'Classic Maya Collapse' (e.g. Culbert, 1973; Webster, 2002), has been a major focus of Maya archaeological research, with proposed causes including extended droughts, greedy rulers, foreign influences, deforestation, and fatalism, among others (Aimers, 2007; Sabloff, 1990; Yaeger and Hodell, 2008). A complex systems perspective, however, suggests that multiple factors over spatial and temporal scales interacted dynamically, affecting both the resilience and the vulnerability of the Maya social-ecological system (e.g. Dunning et al., 2012; Luzzadder-Beach et al., 2012; Turner, 2010). In contrast to identifying a single, isolated overarching trigger of change, this chapter presents a simulation model where biophysical and anthropogenic processes are integrated in order to test hypotheses regarding social-ecological resilience. In demonstrating that no one factor can be singled out as the cause of major transformation, the model supports previous research that has indicated that there were multiple underlying causes for the Maya collapse that varied both spatially and temporally (Chase and Chase, 2004, 2006; Sabloff, 1990; Turner and Sabloff, 2012; Webster, 2002).

We propose a hypothetical framework for how the Maya social-ecological system functioned and represent this system in a simulation model. Qualitative flow diagrams of the ancient Maya system are found in the literature (e.g. Cioffi-Revilla and Landman, 1999; Gunn and Adams, 1981), but their function and the outcomes of several parameters interacting over time have not been tested in a computer-based simulation. In this chapter we describe an integrated modelling approach to operationalize these concepts. Complex systems models represent the connected functional units of a system, with mathematically defined relationships between these units. The resulting simulation is run comparatively under different parameter configurations, and the results tested against archaeological data. The version of the 'MayaSim' model outlined here represents a proof-of-concept model and requires refinement and calibration with archaeological data in further modelling efforts.

The research reported here is an ongoing initiative under the Integrated History and Future of People on Earth project (IHOPE), which builds integrated models of past human societies and their interactions with the environment to yield new insights into those interactions, ultimately to inform planning a more sustainable and desirable future (Costanza et al., 2007, 2012; Crumley, Chapter 1; van der Leeuw et al., 2011), and forms part of the work carried out by the IHOPE-Maya group (Chase and Scarborough, 2014).

From this vantage point, modelling applied to the ancient Maya poses a number of research questions for initial exploration:

- How did past societies impact their environment and respond to changing conditions?
- What relationships between anthropogenic and biophysical processes contribute to resilience or introduce vulnerability, and which indicators best explain the reorganization of past societies?
- What modelled assumptions generate characteristics of the three main Maya temporal periods: the Preclassic (1000 BC–AD 250), Classic (AD 250–900), and Postclassic (AD 900–1500)? Why were major centres located where they were? Why were they dominant when they were?

This chapter describes a novel use of integrated agent-based, cellular automata, and network models (further described in what follows) as a series of programmed modules that represent the building blocks of the Maya social-ecological system, including demographics, trade, agriculture, soil degradation, provision of ecosystem services, climate variability, hydrology, primary productivity, and forest succession. Simulating each of these building blocks in combination allows patterns to emerge at the landscape level, effectively growing the social-ecological system from the bottom up. This approach constructs an artificial social-ecological laboratory where different theories can be tested and hypotheses proposed for how the system will perform under different configurations.

Background and Previous Research

The ancient Maya reorganization defines the transition from the Classic to Postclassic period at a time when Maya society was growing at its fastest rate, building many of its most impressive monuments, and increasing in its socioeconomic connectivity. For instance, Temple IV at Tikal (nearly 65 m in height), the tallest building in the pre-Columbian Americas, was constructed in AD 747 during the apogee of the Late Classic period (Harrison, 1999), and the largest building in current-day Belize is still the main Maya architectural complex of Caana at Caracol, abandoned around AD 900. At the end of the Classic period the population of the Maya lowlands had reached an order of magnitude larger than the region supports today, with some estimates upwards of 10 million people (Rice and Culbert, 1990). In general, Classic Maya cities were organized as a series of extensive and complex agro-urban landscapes (Isendahl, 2012), with low urban population density but with high population density at the landscape level (D. Chase et al., 2011: 65–66). Although the leadership of Maya polities and cities spent massive amounts of resources and energy on conspicuous consumption and monumental construction (Lentz and Hockaday, 2009), the Maya also invested in transforming the landscape to manage natural resources—such as water and soil—allowing the enhancement and sustainability of agricultural production levels (Beach et al., 2002, 2009; Chase and Chase, 1998a; A. Chase et al., 2011; Ford and Clarke, Chapter 9; Isendahl et al., Chapter 26; Luzzadder-Beach and Beach, 2009; Luzzadder-Beach et al., 2012; Scarborough and Lucero, 2010).

Following their Late Classic peak, there was a political, social, and economic crisis, and many small, medium-sized, and large cities—some supporting upwards of 80,000 to 100,000 people—were abandoned (Guderjan et al., 2009; Turner and Sabloff, 2012). In some locations the process extended over as much as 200 years. Although the Maya had successfully dealt with shocks such as droughts for many centuries before the Postclassic transition and had rebounded after adversity, the gravity of the societal reorganization at this time was different in its impact (Luzzadder-Beach et al., 2012; Scarborough and Burnside, 2010). Evidence from palaeoenvironmental records suggests climate instability around the same time as Maya polities were at peak demographic and integrative levels (e.g. Iannone, 2014). Palaeoclimatic proxy records reveal long-term declines in both rainfall and an increase in inter-annual variation (Hodell and Guilderson, 2001).

We hypothesize that although the Maya were at their 'peak' in terms of population, construction, consumption levels, and connectivity between urban areas, the resilience of the social-ecological system was eroded. Dunning et al. (2012: 3652) measure resilience via 'three factors … options for change, system rigidity, and resilient capacity'. Luzzadder-Beach et al. (2012: 3646) define collapse as 'enduring social, political, and economic decline for multiple human generations', noting that Tainter (2000) defines a time period for societal collapse as 'pronounced decline … within two or three generations' (Dunning et al., 2012: 3652). In order to test this argument, quantitative metrics of resilience are required. These can be designed and tested in simulation models.

The first step to designing a complex systems model is defining the critical functional elements of the system, in this case assumed to include water (Scarborough, 2006; Scarborough and Lucero, 2010), infrastructure (Chase and Chase, 1992; D. Chase et al., 2011), climate variation (Gunn et al., 2002; Lucero et al., 2011; Medina-Elizalde and Rohling, 2012), trade and transport (Chase and Chase, 1989; McKillop, 2010), ecology and ecosystems services (Fedick, 1996; Lentz, 2000), agriculture (Harrison and Turner, 1978), population and demographics (Culbert and Rice, 1990), governance and institutions (Marcus, 1993; Martin and Grube, 2000), and war and foreign intervention (Chase and Chase, 1998b; Webster, 2000).

Methods

The MayaSim model is constructed using the software NetLogo (Wilensky, 1999), and represents interactions of three basic functional units: (1) cellular space, (2) agents that operate on top of cells, and (3) network links that connect agents. Although the model uses cells and networks, the principal set of functions apply to agents representing Maya settlements and hence this model is referred to as an agent-based model. Each of the cells, agents, and links contains an array of parameters, and the overall model contains equations with variables using these parameters. A simulation event sequence organizes the execution of the equations and tracks results. The model interface of the software, shown in Fig. 16.1, presents the spatial view of the model with figures tracking model data and a 'control panel' for interacting with the model. The view can be changed to observe different spatial data layers within the model.

Agent-based modelling (ABM) is the computational study of systems of interacting autonomous entities, each with dynamic behaviour and heterogeneous characteristics (Heckbert et al., 2010). The 'agents' interact with each other and their environment within spatially-explicit simulations, resulting in emergent outcomes. Interactions can be direct such as communication and physical interaction by mobile agents in space, or indirect via feedbacks from aggregate outcomes such as environmental feedbacks from the spatial landscape (Heckbert and Bishop, 2011). This style of modelling is different from more commonly used kinds of modelling in archaeology, such as GIS-based data visualization, statistical modelling, or top-down aggregated systems modelling.

The model sequence organizes the execution of functions for settlements, cells, and network links. These events are organized into two categories, with functions relating to biophysical processes and functions relating to anthropogenic processes, as outlined in Table 16.1 and further described in the following sections. A technical description of model equations is presented in Heckbert (2013).

Imported spatial data include elevation and slope (Farr et al., 2007), soil productivity (FAO et al., 2009), and temperature and precipitation (Hijmans et al., 2005). Data are resampled at a 20 km2 resolution using the NetLogo GIS extension (see Wilensky, 1999).

Biophysical Variables

Spatial data for precipitation and temperature represent current conditions (1950 to present day), and are adjusted within the model using simple assumptions which oscillate between higher and lower total precipitation, and vary along a diagonal gradient from south-east (higher precipitation) to north-west (lower precipitation) based on Folan et al. (1983) and Williams (1976) which serves to pronounce the climate variation effect towards the north-west. Future versions will incorporate empirically-based palaeoclimatic reconstructions; however, this proof-of-concept version simplifies the pattern to represent a diagonal north–south/west–east variation in rainfall. Rainfall cycles from + 20 per cent to –10 per cent over a 56 time step cycle. A time step represents about three years, and a complete model run totals 650 time steps, or about 1,950 years. The time resolution is variable, and Heckbert (2013) presents an updated version running at 10-year time steps. The climate variation function serves to reduce and increase rainfall cyclically, with a more pronounced effect further towards the north-west.

The tropical environment of the Maya lowlands is heterogeneous and the region has a seasonal dry-period and karst limestone geological structure, with these factors

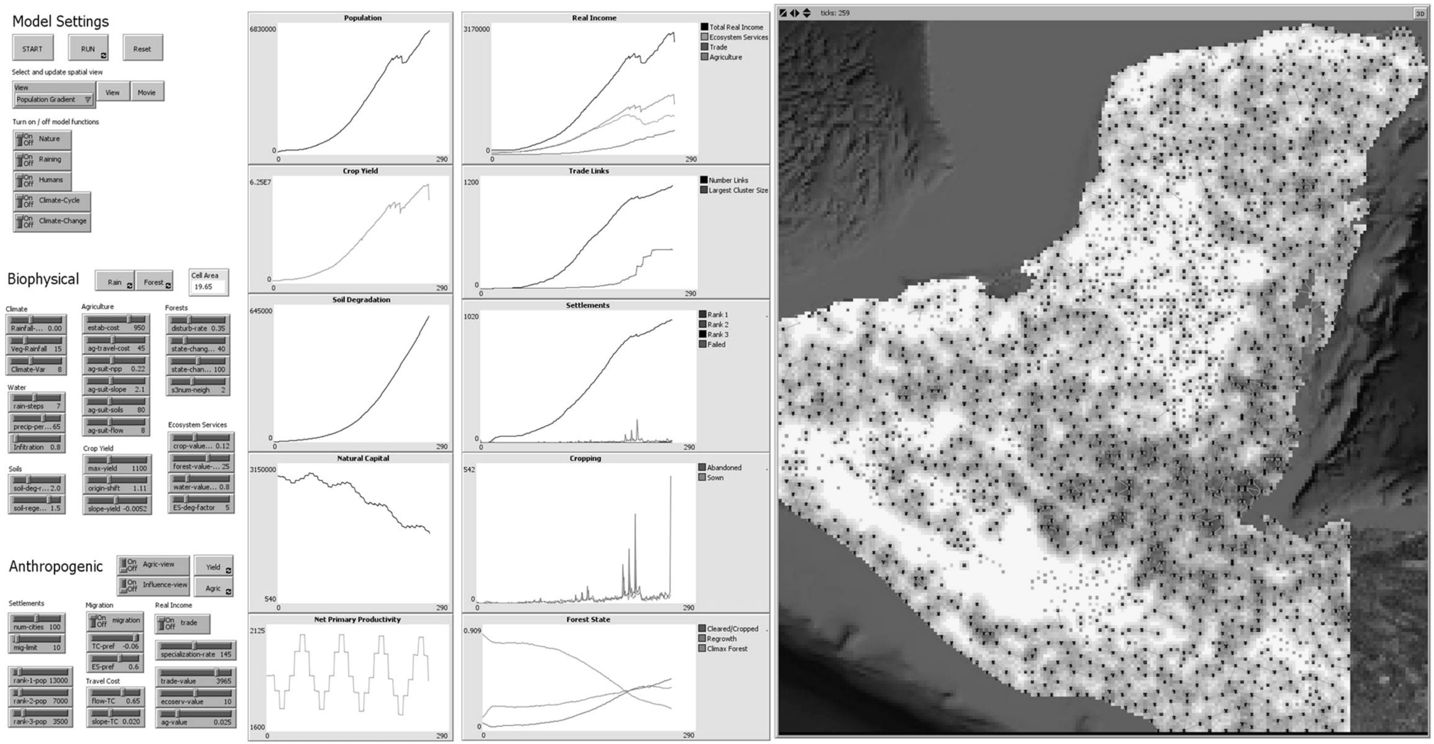

FIGURE 16.1 MayaSim model interface with interactive controls, spatial view, and figures tracking model data. Agents operate on a GIS-based cellular landscape and are connected by links within a network. Time series data are displayed for relevant indicators, and parameter settings can be adjusted to run comparative scenarios.

Photos from the author

Table 16.1 Event sequence for biophysical and anthropogenic processes executed each time step

Module	Event sequence	Function name	Description
Biophysical	1	Climate-variation	Varies rainfall on diagonal north-west gradient
	2	Rain-surface-flow	Calculates water flow
	3	Net-primary-prod	Calculates net primary productivity
	4	Forest-succession	Forest succession modelled as cellular automata
	5	Soil-degradation	Cropped cells incur degradation
	6	Ecosystem-services	Subset of ecosystem services calculated from water, soil, and forest conditions
Anthropogenic	7	Agriculture	Benefit–cost of sowing and abandoning individual crops and calculation of total settlement yield
	8	Demographics	Birth, death, migration, and founding of new settlements
	9	Population-density	Calculates population density gradient
	10	Travel-cost	Calculates 'friction' of cells
	11	Trade	Arranges settlements in networks and calculates trade values
	12	Real-income	Agriculture, ecosystem services, and trade combine for total real income per person for each settlement

playing out differently in different subregions. In several areas of the southern lowlands, rivers played an important part in transport systems, for freshwater procurement, and in riverine agriculture. Other forms of wetland agriculture were also important in the same region and in the north-east of the peninsula (Beach et al., 2009). In parts of the southern lowlands agriculture was organized around extensive seasonal wetland depressions, called *bajos* (Dunning et al., 2006). However, in many other areas climate and the karst environment interacted to prevent rivers and large standing bodies of water developing, and the Maya invented a series of agrosystems and water management strategies to address water deficiency (Isendahl et al., Chapter 26).

Today's landscape is notably different than that of the ancient Maya. Changing land-use, settlement patterns, and biophysical processes such as sea-level rise (Beach et al., 2009) have contributed, and continue to contribute, to altered hydrological dynamics. Therefore, a hydrological model was devised to recreate past conditions simply based on elevation and rainfall. These data are used to calculate surface flow and location of potential seasonal standing water. Each cell generates a mobile 'raindrop' containing a given precipitation volume. The raindrops follow the elevation data, moving to the adjacent cell with the lowest elevation (and considering the summed volume [mm] of raindrops already at that location). If raindrops cannot move (i.e. a location is flooded), the raindrops 'pool' and form river and lake patterns. This flow pattern can be validated against GIS-based methods. The function serves to move water based on elevation, and can simulate the spatial distribution and flow rates of rivers and lakes, as shown in Fig. 16.2. The result of these equations is a surprising spatial pattern that is able to recreate the potential river, lake, and wetland systems under climate variation assumptions. An important caveat of the model output, however, is that surface water in many areas drains rapidly to the aquifer owing to significant karst solution of the limestone bedrock, which is a topic for further research effort. Groundwater is a significant component of water supply for ancient Maya wetland agricultural fields in north-western Belize, and for domestic and agricultural water supply on the north-western Yucatan Peninsula (Luzzadder-Beach, 2000; Luzzadder-Beach and Beach, 2009; Isendahl et al., Chapter 26). Furthermore, Beach et al. (2008) show that land-use intensity caused some slopes to change from karstic (infiltration dominant) to fluvial (run-off dominated) during past and modern times.

Under the climate variation assumptions, the model generates rainfall and water flow surfaces as shown in Fig. 16.3. These surfaces serve as inputs for further calculations for model functions, described in the next section.

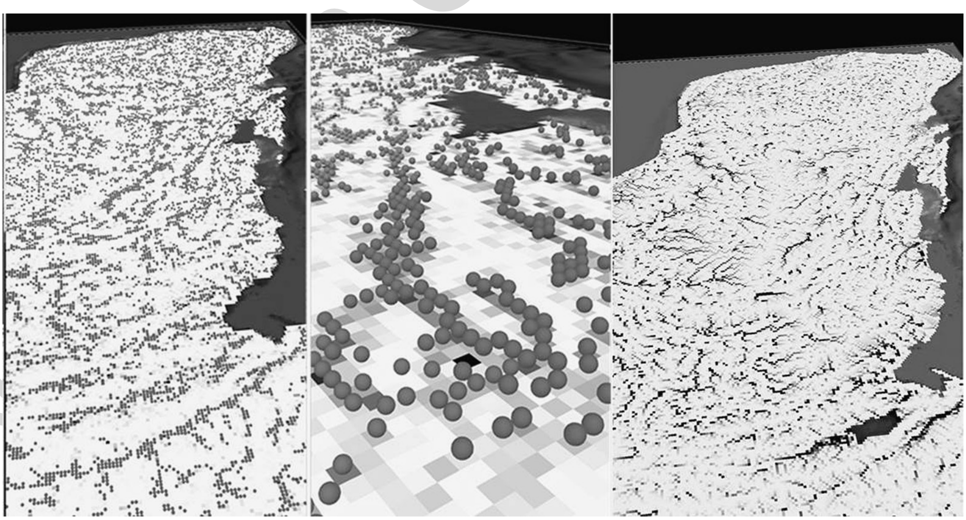

FIGURE 16.2 3D views of 'raindrop' agents following the elevation contour of the landscape to recreate rivers, lakes, and wetlands (left and centre). Movement and interaction of agents generate surface water flow (right) that varies under climate assumptions.

Photos from the author.

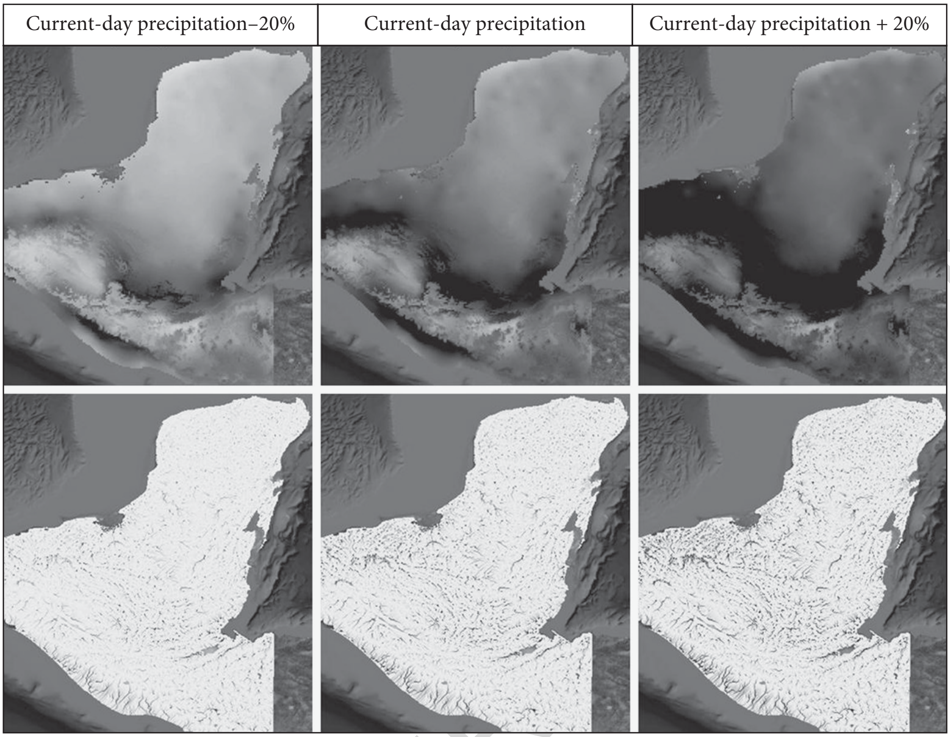

FIGURE 16.3 Spatial model results for the scenario where trade is enabled. Population density, forest condition, and settlement trade strength is shown at time step 200, 400, and 600. Darker shading shows increased population density (top) and trade strength (bottom), and forest condition depicts three states of cleared/cropped cells (lightest), secondary regrowth (middle shading), and climax forest (darkest).

Photos from the author

The base biophysical layers for rainfall and water flow are used to calculate net primary productivity, which in turn is used to calculate forest succession. GIS-based soils data are used to calculate agricultural productivity, and all these combine to calculate provision of ecosystem services. While we recognize that these relationships are complex, simplifying assumptions allow initial representations as methodologies are further refined.

Forest succession operates as a cellular automata model, where the state of a cell is dependent on internal conditions and is influenced by the condition of neighbouring cells. In this proof-of-concept stage, cells take on one of three general forest states that represent climax forest, secondary regrowth, and cleared land, referred to as state 1, 2, and 3 respectively. The forest state is decremented randomly at 3.5 per cent to represent natural disturbance, which is amplified by increased population of nearby settlements to represent fuel and construction wood harvesting (Lentz and Hockaday, 2009). Cells advance in their forest state based on the time since last disturbance. Once the time since last disturbance is above a threshold (40 years for secondary regrowth and 100 years for climax forest) the forest converts to the new state. For conversion to climax forest, a cellular automata function is applied that requires a number of neighbouring cells to also contain climax forest. This rule represents the need to have local vegetation for seed dispersal.

Net primary productivity is a function of precipitation and temperature, which in turn contributes to the calculation of agricultural productivity. Further model refinement will use an agronomic crop production model that is calculated on the basis of Maya agrosystems. Future research will need to consider other forms of land degradation specific to the Maya lowlands, for instance soil phosphorus dynamics (Dunning and Beach, 2010; Dunning et al., 2012; Lawrence et al., 2007; Perez-Salicrup, 2004; Turner, 2010).

Ecosystem services are modelled by quantifying the availability of freshwater, forest resources, and arable land. Dearing et al. (2010) outline a categorization of ecosystem services and identify suitable palaeoenvironmental records for tracking changes in ecosystem services. Our current simplified ecosystems services equation incorporates a subset of four important ecosystem services: arable soils, rainfall, access to available freshwater, and forest resources.

Anthropogenic Variables

Each settlement agent maintains at least one cell for generating agricultural yield. Settlements perform an agriculture benefit–cost assessment considering the costs of production, travel cost given the distance of the cell from the settlement site, and with larger settlements achieving economies of scale. The agriculture function generates yields that are spatially distributed based on individual conditions of the cells. Costs of production are determined by distance from settlements and agricultural productivity, and adding cropped cells generates yield but causes soil degradation. The system adjusts over time in response to the spatially-explicit agricultural benefit–cost.

A series of functions represent trade within a spatially connected network of agents. It is assumed that through the process of specialization and economic diversification, settlements that are connected to one another via a network of spatial interaction will generate benefits from trade. It is assumed that the larger the network, the larger the trade benefit; and also the more central a settlement is within the network, the higher benefits for that individual settlement. To model these benefits, settlements are connected via a network of links that represent trade routes. As a simplifying assumption of how they connect together, we assume when a settlement reaches (or drops below) a certain size, they will add routes (or allow routes to degrade) to nearby settlements within a reasonable distance (we assume 40 km, though Chase and Chase [1998b] reported Maya polities could effectively control a territory with a 60 km radius based on marching distance and military theory), and be weighted towards connecting with wealthier settlements. From this network, settlements calculate the centrality and the size of their local network.

Combining the functions for agriculture, ecosystem services, and trade benefit results in total real income per capita. The value of each contribution to real income is determined by a weighting parameter which is static for agriculture and ecosystem services. The value of trade is, however, dynamic. Specifically, trade value increases each time rainfall decreases, according to the climate variation assumptions. The assumption here is that settlements specialize production within an overall trade network to increase the value of trade goods relative to other commodities. This also partially addresses investment in landesque capital for economic intensification such as infrastructure. The effect is to linearly increase the value of trade each time the climate cycle is in decline. This assumption is obviously rudimentary, and further formulations are explored.

After determining real income levels, settlement demographics account for births, deaths, and migration. The birth rate is assumed to remain constant at 15 per cent, while death rate and out-migration decrease linearly with increased real income per capita. Settlements with a population below a minimum number required to maintain subsistence agriculture are deleted. Settlements that register out-migration above a minimum threshold of the number of people required to maintain subsistence agriculture create a 'migrant agent'. The migrant agent uses a utility function to select locations to create a new settlement (for other applications see Baynes and Heckbert, 2010; Heckbert et al., 2010).

Results

Fig. 16.4 depicts population density, forest condition, and trade strength, viewed at time steps 200, 400, and 600. By time step 200, settlements have expanded into all regions, again first occupying areas with high levels of ecosystem services and progressively growing through agriculture development. Population densities are somewhat higher in areas where settlements have clustered and formed local trade connections. By time step 400, as the value of trade increases, the population has dramatically increased, extending local trade connections to 'global' connectivity. A notable fringe exists between the connected network and the periphery. The centre of the global trade network is approximately in the broad region where the major ancient Maya urban centres of Tikal and Caracol were located. The condition of the forest is markedly changed, with only small patches of climax forest remaining in agriculturally unsuitable areas, forming ecological refugia within the near-completely settled landscape. Dramatically, by time step 600 the trade network has disintegrated, the centre of the most densely populated areas is nearly entirely abandoned, leaving only a small number of locally connected settlements of any notable size in what was once the fringe of the globally connected network. Abandoned cropland and significantly decreased fuelwood harvesting allows broad-level secondary regrowth, and climax forest eventually expands out from its refugia to an extent similar to pre-population expansion levels.

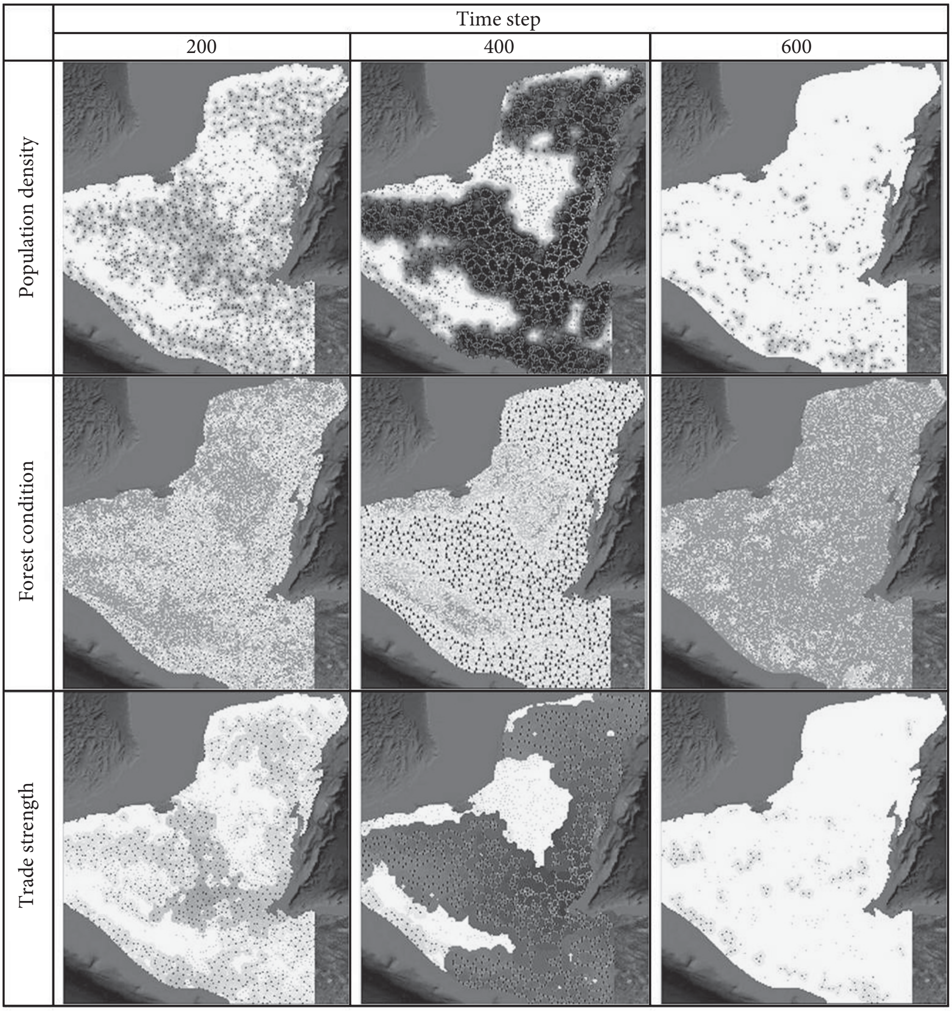

FIGURE 16.4 Spatial model results for the scenario where trade is enabled. Population density, forest condition, and settlement trade strength is shown at time step 200, 400, and 600. Darker shading shows increased population density (top) and trade strength (bottom), and forest condition depicts three states of cleared/cropped cells (lightest), secondary regrowth (middle shading), and climax forest (darkest).

Photos from the author.

The dynamics of this dramatic reorganization can be further investigated using the model to report on quantitative indictors through time, and also by drilling down into each of the model components of demographics, ecosystem services, agriculture and soil degradation, trade links and network connectivity, and forest condition.

Fig. 16.5 depicts results for total population, with the secondary y axis reporting the total summed ecosystem service value for all landscape cells. Here we see that although population numbers were at a 'peak', the value of natural capital was at a 'low'.

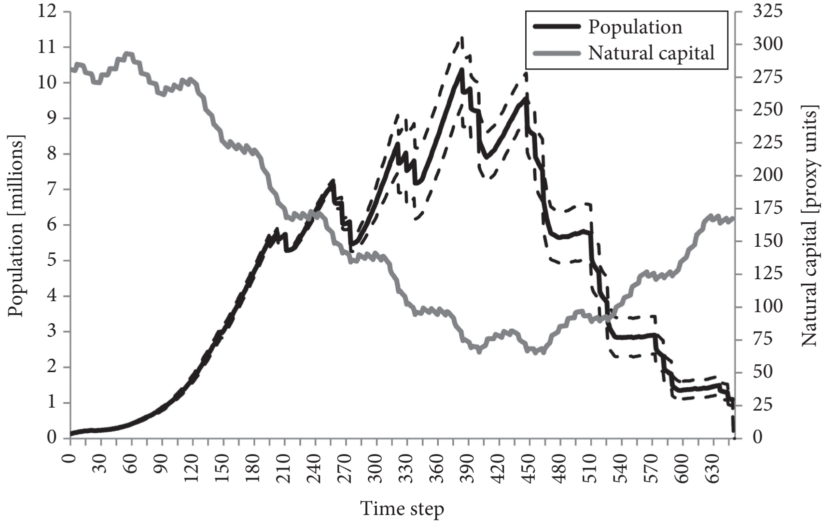

FIGURE 16.5 Total population of all simulated settlements over time, and total ecosystem services of landscape cells. Although the population is at its peak around time step 400, natural capital is at its lowest levels.

Figure from the author

Fig. 16.6 breaks down the components of real income. The timeline for contributions to real income is different for ecosystem services, agriculture, and trade. Initially population growth is fuelled by access to abundant ecosystem services. By time step 200 population pressure begins to degrade ecosystem service values and agriculture development maintains population growth. By time step 300 trade has overtaken ecosystem services in terms of contribution to real income and increases near-exponentially, overtaking agriculture as well.

The dynamics of trade value is dependent on the underlying trade network structure. Each settlement is a potential node in the network, and the configuration of links depends on the settlements' (and their neighbours') size over time. Migration, soil degradation, and climate variation serve to perturb the network, and several links may be deleted and reformed amongst settlements over the course of a climate cycle. Over time settlements that persist in good agriculture areas form stable network links. The development of these links forms clusters used to calculate trade strength. There is a threshold where the number of nodes versus links allows the network to become near-globally connected, as shown in Fig. 16.7 which presents the total number of links between settlements, and the size of the largest cluster. This explains the dramatic increase in trade value observed in Fig. 16.6, as the fast and slow perturbations in the network serve to give it a resilient structure, and the increased value of trade drives growth which serves to extend local clusters to global connectivity.

Given that demographics is driven in this model by real income per capita, the increase in trade value results in an increase in population. To keep up with population growth, settlements plant additional crops in more distant and marginal areas, but also gain

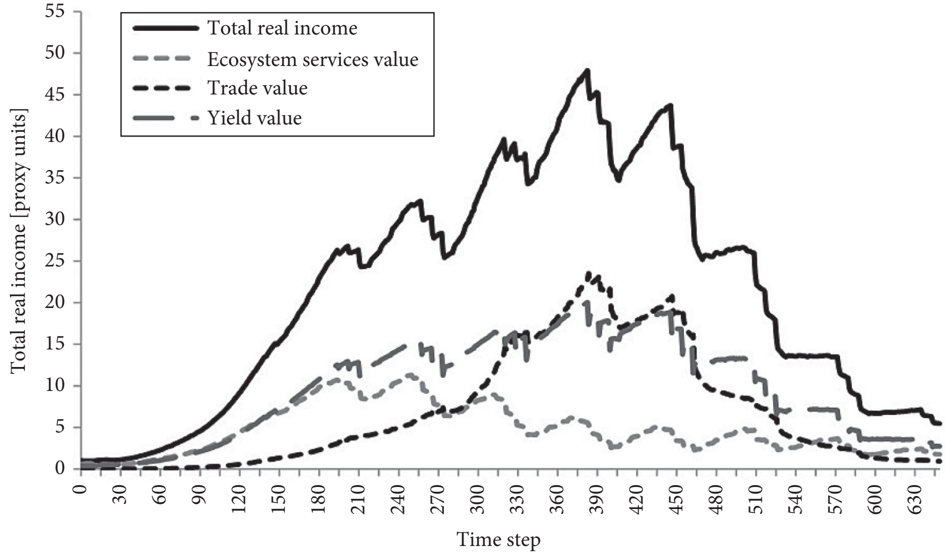

FIGURE 16.6 Real income of all simulated settlements over time by contributions from agriculture, ecosystem services, and trade value. Ecosystem services are superceded by agriculture at an early stage, and trade dominates after time step 350.

Figure from the author.

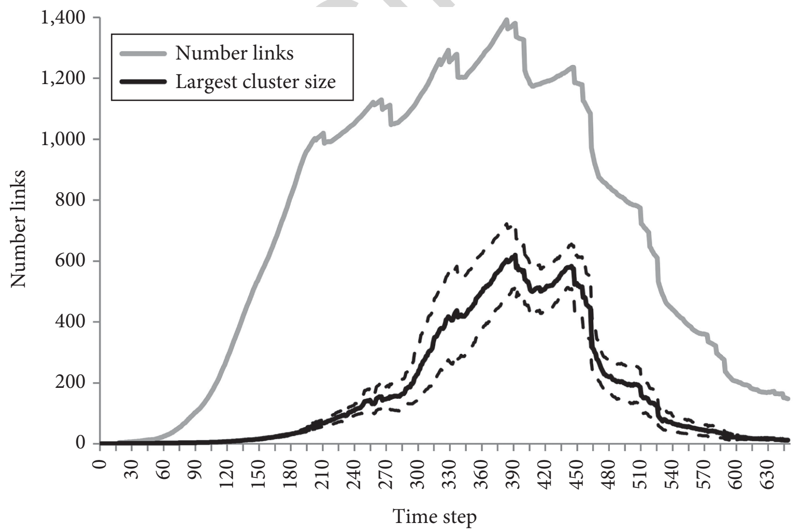

FIGURE 16.7 Trade network structure, reported as the total number of links, and the size of the largest cluster over time. The network grows from local clusters to a near-globally connected system through growth in link connections and periodic perturbations which give the clusters structure.

Figure from the author.

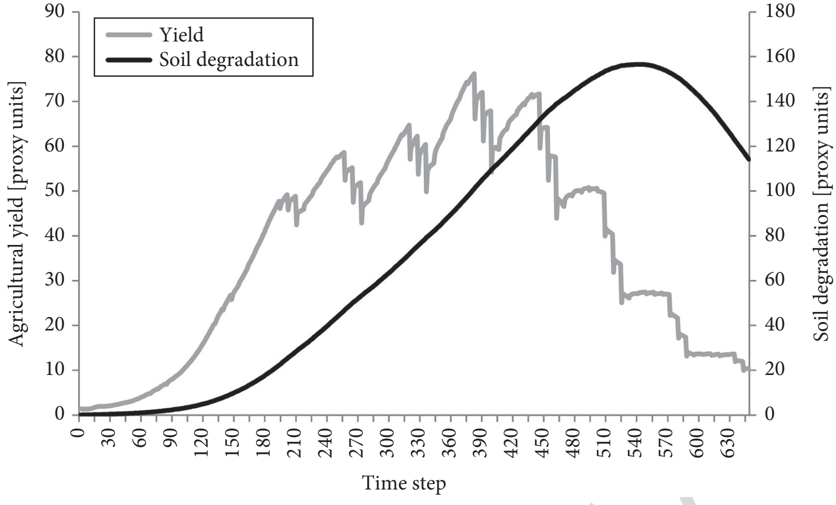

FIGURE 16.8 Agricultural yield and soil degradation simulated over time. After approximately time step 400, soil degradation diminishes yields in relation to population levels.

Figure from the author.

economies of scale making agriculture somewhat 'cheaper'. The result is depicted in Fig. 16.8, tracking agricultural yield and soil degradation. Yield increases in a pattern similar to the population levels in Fig. 16.5, but not at a 1:1 ratio. At around time step 400 soil degradation begins to limit yield and the returns from agricultural investment diminish.

The forest condition is depicted in Fig. 16.9, showing an initial period to time step 200 where climax forest is on a gradual decline, being replaced about evenly by either secondary regrowth or cleared land. After time step 200 the area of cleared land continues to increase, secondary regrowth is depressed, and climax forest is reduced to less than 10 per cent of land area. After time step 400, regrowth is no longer suppressed, large areas reforest, and at approximately year 500 climax forest once again increases.

Discussion and Conclusions

This proof-of-concept agent-based model represents key elements of the ancient Maya social-ecological system. The building blocks of agents, cells, and networks are programmed to represent demographics, trade, agriculture, soil degradation, ecosystem services, climate variability, hydrology, primary productivity, and forest succession. Simulating each of these building blocks in combination allows patterns to emerge at the landscape level, effectively growing the social-ecological system from the bottom up. This allows investigation of how past societies impacted their environment (and vice versa), and permits an examination of what factors contribute to resilience or bring vulnerability, thereby shedding light on why the major centres of the ancient Maya were located where and when they were.

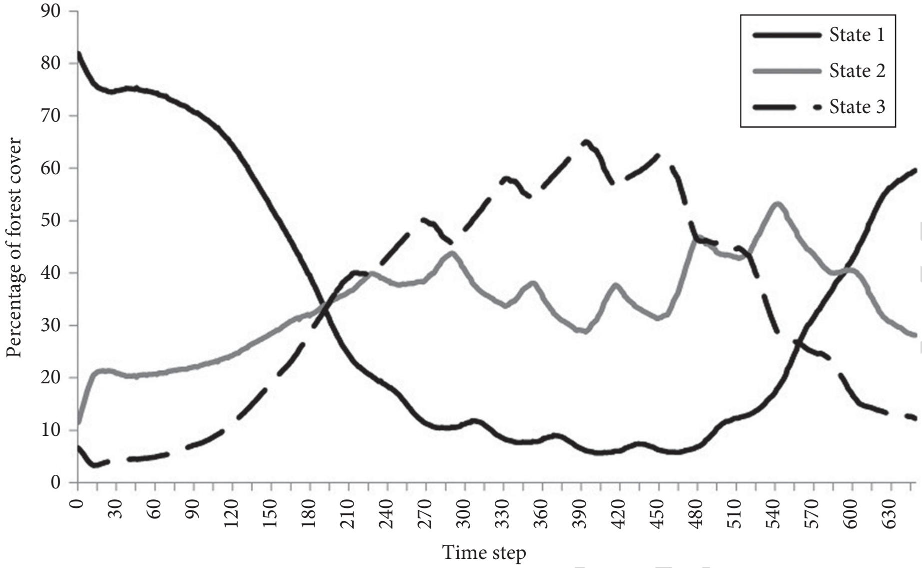

FIGURE 16.9 Forest condition by three states of cleared/cropped cells (state 3), secondary regrowth (state 2), and climax forest (state 1). Accelerated decline of climax forest and inhibited regrowth is a result of cropping as well as demands for construction and fuelwood harvesting.

Figure from the author.

During the verification process, it was observed that model outcomes were particularly sensitive to the relationship between soil degradation and the rate of increase in trade value, again within the range of climate variation. The relationship lies in the fact that settlements with higher per capita real income, due to trade flows, increase in population and more marginal lands are put under production. The population scaling factor for cities then allows for maintaining a higher agricultural area per person than settlements without trade. This in turn increases soil degradation, and thus the relationship between soil productivity and the net value of trade. Independent of our research and results described herein, a social networking study conducted by Golitko et al. (2012) suggests that disruptions in trade linkages during the Late Classic were indeed pivotal in inciting socioeconomic reorganization.

The verification process also identified that the Maya social-ecological system, under given assumptions, does not necessarily reach a 'peak' as observed in the prehistorical record, without a relative balance in the set of parameters relating to trade, ecosystem services, and agricultural wealth. In fact, observing a 'peak' is the exception rather than the norm (across multiple simulation runs), suggesting that biophysical, economic, and demographic conditions needed to be 'just right' in order to allow the Maya to reach their height of social complexity. The two primary parameters that seem to require balance are the increase in trade value and the rate of soil degradation. But note that both are second derivatives, with trade value being a 'fast' variable, and soil degradation being a 'slow' variable. An analogy is that trade is the fire and soil productivity is the fuel—a roaring fire consumes the fuel quickly and extinguishes more rapidly.

As seen in Figs. 16.5, 16.8, and 16.9, with population decline, the rate of soil loss stabilizes and forest recovers relatively rapidly, a prediction that matches well with empirical data from the Maya lowlands (e.g. Mueller et al., 2010). However, the modelled rate of soil recovery after degradation (1 per cent per time step) in reality might be much slower, perhaps taking millennia, and may factor into the slow rate of reoccupation in some regions and the fact that many areas still have truncated and thus diminished soil profiles (Beach et al., 2008; Dunning et al., 2012).

Further research will focus on calibrating model inputs from agronomic models, inputting finer resolution soil and vegetation data, testing alternative functional assumptions, and running the model over a generated palaeoclimate reconstruction. Validation procedures will be more appropriate and rigorous after additional calibration efforts. This will entail comparing model outputs for settlement location and population size over time, as well as land-use changes as indicated through sediment coring, and the evaluation of settlement connectivity as evidenced through ceramic assessments reflective of the kinds and degrees of social exchange and interactions by the ancient Maya. Further contributions to quantifying resilience will use the model as a predictor of reorganization. Candidate statistics include the fluctuation in trade value at the network fringes, the fragility of central nodes in global networks, and the difference in the derivatives of soil productivity and number of nodes versus links; in other words the rates at which slow and fast variables interact, which can cause a 'resonance' that exhausts the system.

Acknowledgements

The authors would like to acknowledge the National Center for Ecological Analysis and Synthesis, Portland State University, Arizona State University, the World Historical Ecology Network, Uppsala University, and University of Cincinnati. All illustrations have been produced by the senior author.

References

Aimers, J. J. (2007). What Maya collapse? Terminal Classic variation in the Maya Lowlands. *Journal of Archaeological Research* 15(4): 329–377.

Baynes, T., and Heckbert, S. (2010). Micro-scale simulation of the macro urban form: opportunities for exploring urban change and adaptation. *Lecture Notes in Computer Science* 5683: 14–24.

Beach, T., Luzzadder-Beach, S., Dunning, N., and Cook, D. (2008). Human and natural impacts on fluvial and karst depressions of the Maya lowlands. *Geomorphology* 101(1–2): 301–331.

Beach, T., Luzzadder-Beach, S., Dunning, N., Hageman, J., and Lohse, J. (2002). Upland agriculture in the Maya lowlands: ancient conservation in northwestern Belize. *The Geographical Review* 92(3): 372–397.

Beach, T., Luzzadder-Beach, S., Dunning, N., Jones, J., Lohse, J., Guderjan, T., Bozarth, S., Millspaugh, S., and Bhattacharya, T. (2009). A review of human and natural changes in Maya lowlands wetlands over the Holocene. *Quaternary Science Reviews* 28(17–18): 1710–1724.

Chase, A. F., and Chase, D. Z. (1989). Routes of trade and communication and the integration of Maya society: the vista from Santa Rita Corozal. In H. McKillop and P. Healy (eds), *Coastal Maya Trade*. Toronto: Trent University, 19–32.

Chase, A. F., and Chase, D. Z. (1998a). Scale and intensity in Classic Period Maya agriculture: terracing and settlement at the 'garden city' of Caracol, Belize. *Culture and Agriculture* 20(2–3): 60–77.

Chase, A. F., and Chase, D. Z. (1998b). Late Classic Maya political structure, polity size, and warfare arenas. In A. Ciudad Ruiz, M. Y. Fernández Marquínez, J. M. García Campillo, M. J. Iglesias Ponce de León, A. Lacadena García-Gallo, and L. T. Sanz Castro (eds), *Anatomia de una Civilizacion: Aproximaciones Interdisciplinarias a la Cultura Maya*. Madrid: Sociedad Espanola de Estudios Mayas, 11–29.

Chase, A. F., and Scarborough, V. L. (eds) (2014). *The Resilience and Vulnerability of Ancient Landscapes: Transforming Maya Archaeology through IHOPE*. Archaeological Paper of the American Anthropological Association, Vol. 24. Hoboken, NJ: Wiley-Blackwell.

Chase, A. F., Chase, D. Z., Weishampel, J. F., Drake, J. B., Shrestha, R. L., Slatton, K. C., Awe, J. J., and Carter, W. E. (2011). Airborne LiDAR, archaeology, and the ancient Maya landscape at Caracol, Belize. *Journal of Archaeological Science* 38(2): 387–398.

Chase, D. Z., and Chase, A. F. (eds) (1992). *Mesoamerican Elites: An Archaeological Assessment*. Norman, OK: University of Oklahoma Press.

Chase, D. Z., and Chase, A. F. (2004). Hermeneutics, transitions, and transformations in Classic to Postclassic Maya society. In A. Demarest, P. Rice, and D. Rice (eds), *The Terminal Classic in the Maya Lowlands: Collapse, Transition, and Transformation*. Boulder, CO: University Press of Colorado, 12–27.

Chase, D. Z., and Chase, A. F. (2006). Framing the Maya collapse: continuity, discontinuity, method, and practice in the Classic to Postclassic southern Maya Lowlands. In G. Schwarts and J. Nichols (eds), *After the Collapse: The Regeneration of Complex Societies*. Tucson, AZ: University of Arizona Press, 168–187.

Chase, D. Z., Chase, A. F., Awe, J. J., Walker, J. H., and Weishampel, J. F. (2011). Airborne LiDAR at Caracol, Belize and the interpretation of ancient Maya society and landscapes. *Research Reports in Belizean Archaeology* 8: 61–73.

Cioffi-Revilla, C., and Landman, T. (1999). Evolution of Maya polities in the ancient Mesoamerican system. *International Studies Quarterly* 43(4): 559–598.

Costanza, R., Graumlich, L., Steffen, W., Crumley, C., Dearing, J., Hibbard, K., Leemans, R., Redman, C., and Schimel, D. (2007). Sustainability or collapse: what can we learn from integrating the history of humans and the rest of nature? *Ambio* 36(7): 522–527.

Costanza, R., van der Leeuw, S., Hibbard, K., Aulenbach, S., Brewer, S., Burek, M., Cornell, S., Crumley, C., Dearing, J., Folke, C., Graumlich, L., Hegmon, M., Heckbert, S., Jackson, S. T., Kubiszewski, I., Scarborough, V., Sinclair, P., Sörlin, S., and Steffen, W. (2012). Developing an integrated history and future of people on earth (IHOPE). *Current Opinion in Environmental Sustainability* 4(1): 106–114.

Culbert, T. P. (ed.) (1973). *The Classic Maya Collapse*. Albuquerque, NM: University of New Mexico Press.

Culbert, T. P., and Rice, D. S. (eds) (1990). *Precolumbian Population History in the Maya Lowlands*. Albuquerque, NM: University of New Mexico Press.

Dearing, J. A., Braimoh, A. K., Reenberg, A., Turner, B. L. II, and van der Leeuw, S. E. (2010). Complex land systems: the need for long time perspectives to assess their future. *Ecology and Society* 15(4): 21.

Dunning, N., and Beach, T. (2010). Farms and forests: spatial and temporal perspectives on ancient Maya landscapes. In I. P. Martini and W. Chesworth (eds), *Landscapes and Societies*. Berlin: Springer-Verlag, 369–389.

Dunning, N., Beach, T., and Luzzadder-Beach, S. (2006). Environmental variability among bajos in the southern Maya lowlands and its implications for ancient Maya civilization and archaeology. In L. Lucero and B. Fash (eds), *Pre-Columbian Water Management: Ideology, Ritual, and Power*. Tucson, AZ: University of Arizona Press, 81–99.

Dunning, N., Beach, T., and Luzzadder-Beach, S. (2012). Kax and kol: collapse and resilience in lowland Maya civilization. *Proceedings of the National Academy of Sciences of the United States of America* 109(10): 3652–3657.

FAO/IIASA/ISRIC/ISSCAS/JRC (2009). *Harmonized World Soil Database (Version 1.1)*. Rome and Laxenburg (Austria): FAO and IIASA.

Farr, T. G., Rosen, P. A., Caro, E., Crippen, R., Duren, R., Hensley, S., Kobrick, M., Paller, M., Rodriguez, E., Roth, L., Seal, D., Shaffer, S., Shimada, J., Umland, J., Werner, M., Oskin, M., Burbank, D., and Alsdorf, D. (2007). The Shuttle Radar Topography Mission. *Reviews of Geophysics* 45(2), doi: 10.1029/2005RG000183.

Fedick, S. (ed.) (1996). *The Managed Mosaic: Ancient Maya Agriculture and Resource Use*. Salt Lake City, UT: University of Utah Press.

Folan, W. J., Gunn, J. D., Eaton, J. D., and Patch, R. W. (1983). Paleoclimatological patterning in southern Mesoamerica. *Journal of Field Archaeology* 10: 453–468.

Golitko, M., Meierhoff, J., Feinman, G. M., and Williams, P. R. (2012). Complexities of collapse: the evidence of Maya obsidian as revealed by social network graphical analysis. *Antiquity* 86(332): 507–523.

Guderjan, T., Beach, T., Luzzadder-Beach, S., and Bozarth, S. (2009). Understanding the causes of abandonment in the Maya lowlands. *Archaeological Review from Cambridge* 24(2): 99–121.

Gunn, J. D., and Adams, R. E. W. (1981). Climatic change, culture, and civilization in North America. *World Archaeology* 13(1): 85–100.

Gunn, J. D., Matheny, R. T., and Folan, W. J. (2002). Climate-change studies in the Maya area: a diachronic analysis. *Ancient Mesoamerica* 13(1): 79–84.

Harrison, P. D. (1999). *The Lords of Tikal: Rulers of an Ancient Maya City*. London: Thames & Hudson.

Harrison, P. D., and Turner, B. L. II (eds) (1978). *Pre-Hispanic Maya Agriculture*. Albuquerque, NM: University of New Mexico Press.

Heckbert, S. (2013). MayaSim: an agent-based model of the ancient Maya social-ecological system. *Journal of Artificial Societies and Social Simulation* 16(4): 11.

Heckbert, S., and Bishop, I. (2011). Empirical calibration of spatially explicit agent-based models. In D. Marceau and I. Benenson (eds), *Advanced Geosimulation Models*. Hilversum, The Netherlands: Bentham, 92–110.

Heckbert, S., Baynes, T., and Reeson, A. (2010). Agent-based modelling in ecological economics. *Annals of the New York Academy of Sciences Ecological Economics Reviews* 1185: 39–53.

Hijmans, R. J., Cameron, S. E., Parra, J. L., Jones, P. G., and Jarvis, A. (2005). Very high resolution interpolated climate surfaces for global land areas. *International Journal of Climatology* 25(15): 1965–1978.

Hodell, D. A., and Guilderson, T. (2001). Solar forcing of drought frequency in the Maya lowlands. *Science* 292(5520): 1367–1370.

Iannone, G. (ed.) (2014). *The Great Maya Droughts in Cultural Context: Case Studies in Resilience and Vulnerability*. Boulder, CO: University Press of Colorado.

Isendahl, C. (2012). Agro-urban landscapes: the example of Maya lowland cities. *Antiquity* 86(334): 1112–1125.

Lawrence, D., d'Odorico, P., Diekmann, L., Delonge, M., Das, R., and Eaton, J. (2007). Ecological feedbacks following deforestation create the potential for a catastrophic ecosystem shift in tropical dry forest. *Proceedings of the National Academy of Sciences of the United States of America* 104(52): 20696–20701.

Lentz, D. L. (2000). Anthropocentric food webs in the Precolumbian Americas. In D. L. Lentz (ed.), *Imperfect Balance: Landscape Transformations in the Precolumbian Americas*. New York: Columbia University Press, 89–120.

Lentz, D. L., and Hockaday, B. (2009). Tikal timbers and temples: ancient Maya agroforestry and the end of time. *Journal of Archaeological Science* 36(7): 1342–1353.

Lucero, L. J., Gunn, J. D., and Scarborough, V. L. (2011). Climate change and Classic Maya water management. *Water* 3(2): 479–494.

Luzzadder-Beach, S. (2000). Water resources of the Chunchucmil Maya. *The Geographical Review* 90(4): 493–510.

Luzzadder-Beach, S., and Beach, T. (2009). Arising from the wetlands: mechanisms and chronology of landscape aggradation in the northern coastal plain of Belize. *Annals of the Association of American Geographers* 99(1): 1–26.

Luzzadder-Beach, S., Beach, T. P., and Dunning, N. P. (2012). Wetland fields as mirrors of drought and the Maya abandonment. *Proceedings of the National Academy of Sciences of the United States of America* 109(10): 3646–3651.

McKillop, H. (2010). Ancient Maya canoe navigation and its implications for Classic to Postclassic Maya economy and sea trade: a view from the south coast of Belize. *Journal of Caribbean Archaeology* 3: 93–105.

Marcus, J. (1993). Ancient Maya political organization. In J. A. Sabloff and J. S. Henderson (eds), *Lowland Maya Civilization in the Eighth Century A.D.* Washington, DC: Dumbarton Oaks, 111–183.

Martin, S., and Grube, N. (2000). *Chronicle of Maya Kings and Queens: Deciphering the Dynasties of the Ancient Maya*. London: Thames & Hudson.

Medina-Elizalde, M., and Rohling, E. J. (2012). Collapse of Classic Maya civilization related to modest reduction in precipitation. *Science* 335(6071): 956–959.

Mueller, A. D., Islebe, G. A., Anselmetti, F. S., Ariztegui, D., Brenner, M., Hodell, D. A., Hajdas, I., Hamann, Y., Haug, G. H., and Kennett, D. J. (2010). Recovery of forest ecosystem in the tropical lowlands of northern Guatemala after the disintegration of Classic Maya polities. *Geology* 38(6): 523–526.

Perez-Salicrup, D. (2004). Forest types and their implications. In B. L. Turner II, J. Geoghegan, and D. R. Foster (eds), *Integrated Land-Change Science and Tropical Deforestation in the Southern Yucatan*. Oxford: Oxford University Press, 63–80.

Rice, D. S., and Culbert, T. P. (1990). Historical contexts for population reconstruction in the Maya lowlands. In T. P. Culbert, and D. S. Rice (eds), *Precolumbian Population History in the Maya Lowlands*. Albuquerque, NM: University of New Mexico Press, 1–36.

Sabloff, J. A. (1990). *The New Archaeology and the Ancient Maya*. New York: W. H. Freeman.
Scarborough, V. L. (2006). An overview of Mesoamerican water systems. In L. Lucero and B. Fash (eds), *Precolumbian Water Management*. Tucson, AZ: University of Arizona Press, 223–235.
Scarborough, V. L., and Burnside, W. R. (2010). Complexity and sustainability: perspectives from the ancient Maya and the modern Balinese. *American Antiquity* 75(2): 327–363.
Scarborough, V. L., and Lucero, L. J. (2010). The non-hierarchical development of complexity in the semitropics: water and cooperation. *Water History* 2(2): 185–205.
Tainter, J. A. (2000). Problem solving: complexity, history, sustainability. *Population and Environment* 22(1): 3–41.
Turner, B. L., II (2010). Unlocking the ancient Maya and their environment: paleo-evidence and dating resolution. *Geology* 38(6): 575–576.
Turner, B. L. II, and Sabloff, J. A. (2012). The classic Maya collapse in the central lowlands: insights about human-environment complexity for sustainability science. *Proceedings of the National Academy of Sciences of the United States of America* 109(35): 13908–13914.
van der Leeuw, S., Costanza, R., Aulenbach, S., Brewer, S., Burek, M., Cornell, S., Crumley, C., Dearing, J., Downy, C., Graumlich, L., Hegmon, M., Heckbert, S., Hibbard, K., Jackson, S., Kubiszewski, I., Sinclair, P., Sörlin, S., and Steffen, W. (2011). Toward an integrated history to guide the future. *Ecology and Society* 16(4): 2.
Webster, D. L. (2000). The not so peaceful civilization: a review of Maya war. *Journal of World Prehistory* 14(1): 65–119.
Webster, D. L. (2002). *The Fall of the Ancient Maya: Solving the Mystery of the Maya Collapse*. New York: Thames & Hudson.
Wilensky, U. (1999). *NetLogo*. Evanston, IL: Center for Connected Learning and Computer-Based Modeling, Northwestern University.
Williams, A. Jr. (1976). The interpretation of rainfall patterns in northern Yucatan utilizing meteorological satellite imagery. *Proceedings of the Association of American Geographers* 8: 15–19.
Yaeger, J., and Hodell, D. A. (2008). Climate–culture–environment interactions and the collapse of classic Maya civilization. In J. Quilter (ed.), *El Nino, Catastrophism, and Culture Change in Ancient America*. Washington, DC: Dumbarton Oaks, 187–242.